PLOS ONE

RESEARCH ARTICLE

Integrated transcriptomic and metabolomic analyses of yellow horn (*Xanthoceras sorbifolia*) in response to cold stress

Juan Wang[1,2], **Jinping Guo**[1,2]*, **Yunxiang Zhang**[1,2], **Xingrong Yan**[1,2]

1 College of Forestry, Shanxi Agricultural University, Taigu, Shanxi, China, **2** Shanxi Key Laboratory of Functional Oil Tree Cultivation and Research, Taigu, Shanxi, China

* jinpguo@126.com

Abstract

Xanthoceras sorbifolia, a medicinal and oil-rich woody plant, has great potential for biodiesel production. However, little study explores the link between gene expression level and metabolite accumulation of *X. sorbifolia* in response to cold stress. Herein, we performed both transcriptomic and metabolomic analyses of *X. sorbifolia* seedlings to investigate the regulatory mechanism of resistance to low temperature (4 °C) based on physiological profile analyses. Cold stress resulted in a significant increase in the malondialdehyde content, electrolyte leakage and activity of antioxidant enzymes. A total of 1,527 common differentially expressed genes (DEGs) were identified, of which 895 were upregulated and 632 were downregulated. Annotation of DEGs revealed that amino acid metabolism, glycolysis/gluconeogenesis, starch and sucrose metabolism, galactose metabolism, fructose and mannose metabolism, and the citrate cycle (TCA) were strongly affected by cold stress. In addition, DEGs within the plant mitogen-activated protein kinase (MAPK) signaling pathway and TF families of ERF, WRKY, NAC, MYB, and bHLH were transcriptionally activated. Through metabolomic analysis, we found 51 significantly changed metabolites, particularly with the analysis of primary metabolites, such as sugars, amino acids, and organic acids. Moreover, there is an overlap between transcript and metabolite profiles. Association analysis between key genes and altered metabolites indicated that amino acid metabolism and sugar metabolism were enhanced. A large number of specific cold-responsive genes and metabolites highlight a comprehensive regulatory mechanism, which will contribute to a deeper understanding of the highly complex regulatory program under cold stress in *X. sorbifolia*.

Introduction

Abiotic stresses unfavorably affect growth and productivity in plants and cause a series of changes at the morphological, physiological, biochemical, and molecular levels [1–3]. Low temperature (LT) is one of the major abiotic stresses in plants that disturbs physiological, cellular, metabolic, and molecular functioning, resulting in severe retardation of plant growth and development, and frequently even death [4]. Cell membranes may become disorganized,

osmotic stress can be altered, proteins may lose activity or be denatured, and high levels of reactive oxygen species (ROS) can damage the oxidation system [5]. Further, ROS can trigger various signaling pathways, such as mitogen-activated protein kinase (MAPK) signal transduction cascades for specific responsive gene expression. ROS are limited or scavenged by antioxidant enzymes, such as superoxide dismutase (SOD), peroxidase (POD), and catalase (CAT) [6]. During cold-stress response, plant cells tend to accumulate a series of osmoregulatory metabolites, including soluble sugars (e.g., sucrose, glucose, and galactose) and low molecular weight compounds (e.g., proline, glycine, and betaine) that enable plants to alleviate osmotic stress and maintain cell turgor, water uptake, and metabolic activity [7, 8].

Numerous studies have demonstrated that cold tolerance is a complex quantitative trait involving multiple regulatory mechanisms and metabolic pathways, and is associated with activities of antioxidant enzymes, expression of cold-responsive genes and transcription factors (TFs), and the concentrations of primary and secondary metabolites [9, 10]. Plants can respond to cold stress through a wide range of transcriptional changes to maintain cellular homeostasis and improve cold tolerance. For instance, previous studies have indicated that the CBF transcriptional network plays a central role in cold response in *Arabidopsis* [11]. Exposing *Arabidopsis* plants to LT can rapidly induce a family of three transcriptional activators (CBF1-3) that specifically bind to the CRT/DRE (C-repeat/dehydration-responsive element) *cis*-acting regulatory element of the promoter region of many cold-inducible genes, present in the promoters of COR15a and COR78/RD29a [12]. Therefore, transcriptome analysis is a powerful technology for gene-expression profile analysis at the whole-genome level that has been used to identify numerous cold-responsive genes from different species, including *Arabidopsis* [13, 14], maize [15, 16], rice [17–19], grape [20], and peach [21]. In response to LT stimuli, plants evolve an array of metabolic responses oriented toward stress avoidance, defense, or resistance depending on the particular stress tolerance. Among all metabolic responses, alterations to primary metabolism are the most evident and involve changes in levels of sugars and sugar alcohols, amino acids, and TCA cycle intermediates, thereby exhibiting general trends in response to cold stress. However, changes in secondary metabolism are more species-specific [22]. At present, metabolomic studies have also been applied to explore metabolites involved in cold-stress regulation in many plants, such as maize [23], spruce [24], orange [25], and *Arabidopsis* [26]. Meanwhile, transcriptomics integrated with metabolomics can contribute to a deeper understanding of the gene-to-metabolite pathways associated with cold stress in plants.

Xanthoceras sorbifolia, commonly known as yellow horn, is a member of the Sapindaceae family and originates in China [27]. It is a woody deciduous shrub or small tree with a lifespan of more than 200 years [28]. Yellow horn is considered an important bio-energy feedstock plant because of the significant concentration of oil in the seed kernel (> 60%), and it may become an energy-sustainable substitute for petroleum. Furthermore, the oil contains unsaturated fatty acids up to 90.9% of the total fatty acids, which have potential health benefits [29]. It is highly resistant to environmental stresses, such as cold, drought, and salt stresses. The chloroplast genome of *X. sorbifolia* has been assembled and characterized [30]. The whole genome of *X. sorbifolia* has been sequenced and assembled recently [31, 32]. There have been some reports on the investigations into *X. sorbifolia* transcriptome, including oil accumulation [33, 34], fertilized ovule development [35], as well as abiotic stresses (e.g., NaCl, ABA and low temperature) [36]. However, few studies have focused on the comprehensive information based on transcriptional and metabolic responses to cold stress in *X. sorbifolia*.

In this study, we integrated the transcriptomic and metabolomic analyses of *X. sorbifolia* seedlings to explore the changes that occur in the transcription and metabolite levels in response to cold stress, and sought to reveal potential links between the expression of cold-responsive genes and metabolites accumulation. Therefore, a gene-to-metabolism network

constructed on the basis of observations of massive transcriptome and metabolome repro-
gramming can further elucidate a comprehensive gene regulatory mechanism that involves
cold-signal perception and transduction, transcriptional regulation, and gene expression.
These findings could provide us with a unique opportunity to gain novel insights into the
molecular mechanisms regulating cold tolerance in *X. sorbifolia*.

Materials and methods

Plant materials and treatments

X. sorbifolia seeds were collected from the same tree (accession number: A099), which had sev-
eral superior traits including high oil content, high yield and a certain resistance to cold stress.
This tree was grown from the breeding base owned by Shanxi Agricultural University (37˚
25ʹN, 112˚34ʹE) in China. Seeds were germinated with the sand-hiding method at 25 ˚C
because the seed coat is thick and hard. After 20 days, seedlings were grown in a greenhouse
(light 25 ˚C for 12 h/dark at 20 ˚C for 12 h; relative humidity of 60% –70%) and regularly
watered under natural conditions for a month. From mid-April to mid-May, the changes in
local temperature are often unstable, and sometimes low temperature (about 4 ˚C) lasts for
one to several days, which can affect the normal growth of *X. sorbifolia* seedling. We thus
hypothesized that the changes should also occur in the transcription and metabolite levels of
X. sorbifolia after cold stress at 4˚C. Healthy and uniform seedlings (height, ~30 cm) were
treated at 4 ˚C at different time points. The leaves of these seedling plants were harvested at 0
(control), 4, 12, and 24 h for transcriptome sequencing, and the same samples of 0 (control)
and 24 h were prepared for metabolite profiling with three biological replicates per treatment.
We selected 24 h as the extreme time point according to the phenotypic changes of *X. sorbifolia*
seedlings after cold treatment compared with control (0h). All samples were frozen in liquid
nitrogen immediately and stored at −80 ˚C until further use.

RNA extraction, cDNA synthesis, and sequencing

Total RNA from each sample was extracted using the TaKaRa MiniBEST Plant RNA Extrac-
tion Kit (TaKaRa, Dalian, China) following the manufacturer's instructions. The concentra-
tion and purity of the extracted RNA was verified by agarose gel electrophoresis (1%) and a
NanoDrop 2000C spectrophotometer (Thermo Fisher Scientific, Wilmington, USA). The
integrity of RNA was assessed with an Agilent Bioanalyzer 2100 (Agilent Technologies, Santa
Clara, USA). Sequencing libraries were created using the NEB Next® Ultra™ RNA Library
Prep Kit for Illumina® following the manufacturer's instructions. Index codes were added to
each sample. The prepared libraries were sequenced on the Illumina HiSeq 2500 platform
(Illumina Inc., San Diego, USA) by Biomarker Technology Corporation (www.biomarker.
com.cn). The raw RNA-Seq data were submitted to www.ncbi.nlm.nih.gov/bioproject/
PRJNA608707.

Transcriptome assembly and function annotation

The transcriptome was assembled from all 12 samples, including 3 control samples and 9 cold-
stressed samples. The clean reads were obtained after removing low-quality reads, adapter
sequences, and reads containing poly-N from the raw data. The high-quality reads were assem-
bled *de novo* into transcripts using Trinity software with the paired-end method. All assembled
unigenes were annotated in Kyoto Encyclopedia of Genes and Genomes (KEGG) [37], Gene
Ontology (GO) [38], Clusters of Orthologous Groups (COG) [39], eggnog [40], Swiss-prot
[41], NR [42], and euKaryotic Orthologous Groups (KOG) [43] using BLAST [44] with E-

value $\leq 1.0 \times 10^{-5}$. Transcription levels for each gene were quantified according to the FPKM (fragments per kilobase of exon per million fragments mapped). The FPKM was calculated by normalizing for the length of the gene and total read number mapped to it [45, 46]. False discovery rate-adjusted P value (FDR) < 0.05 and an absolute value of log2 FC $\geq$ 1 were used as the empirical parameters to identify the differentially expressed genes (DEGs). The KEEG pathway annotation was performed on the KAAS (KEEG Automatic Annotation Serve) website (http://www.genome.jp/tools/kaas/). GO annotation was performed using BinGo (https://www.psb.ugent.be/cbd/papers/BiNGO/Home.html) by assigning the annotation to *Arabidopsis* (P value < 0.05), and networks of enriched GO terms were constructed with Cytoscape 3.7.2. TFs were predicted using the PlantTFDB database (http://planttfdb.cbi.pku.edu.cn/).

Metabolic profiling analysis

Frozen samples were sent to Biomarker Technologies Co., Ltd. (Beijing, China) for extract analysis, metabolite identification, and quantification following their standard procedures and previously described by Chen et al. [47]. Briefly, the samples were dried and ground to powder, and powdered samples were extracted and purified by filtration and centrifugation. The purified solution was injected into the GC-TOF-MS system (Pegasus HT, LECO, San Jose, USA) for analysis. The metabolite separations were performed using an Agilent DB-5MS capillary column (30 m×250 μm×0.25 μm, J&W Scientific, Folsom, USA). Mass spectral data were analyzed using ChromaTOF V4.3x (LECO San Jose, USA), including peak extraction, baseline correction, deconvolution, peak integration, and peak alignment. Metabolites were quantified by comparison to the internal standard values and identified according to the LECO-Fiehn Rtx5 database. The data matrices of identified metabolites from 6 samples were uploaded to the Metaboanalyst (http://www.metaboanalyst.ca/) for statistical and pathway analyses. Differential metabolic features were defined according to fold-change > 1.5, variable importance in projection VIP > 1 of the partial least-squares discriminant analysis (PLS-DA) [48], and statistically significant (P value < 0.05) based on Student's t-test.

Physiological measurements

The leaves were sampled and physiological indices were measured after 0 (control), 4, 12, 24, and 48 h of the 4 ˚C treatment. All assays were conducted with three biological repeats. For measurement of electrolyte leakage (EL), the leaf samples were put into 30 ml distilled water and shaken at room temperature for 3 h. The initial conductivity (E1) was measured using a digital conductivity meter. Then, the samples were boiled for 30 min and cooled to room temperature, the final electrolyte conductivity (E2) was measured. Electrolyte leakage (%) = (E1/E2) × 100. The malondialdehyde (MDA) accumulation was measured by the thiobarbituric acid (TBA) colorimetric method using an MDA assay kit (Solarbio, Beijing, China). The content of MDA was expressed as μmol MDA per gram FW.

Activities of SOD, POD, and CAT were determined according to instructions from commercially available kits (Solarbio, Beijing, China). Fresh leaves (0.5 g) were ground to a fine powder in liquid nitrogen, and enzymes were extracted using extraction buffer. Subsequently, the extraction was centrifuged at 8,000 × g for 10 min at 4 ˚C, and the supernatant was used for further experiments. The final reacted solutions were determined using spectrophotometry at 560 nm (for SOD activity), 470 nm (for POD activity), and 240 nm (for CAT activity). All measurements were performed according to the instructions of the antioxidant enzyme assay kit. The enzyme activities were expressed as units of enzyme activity per gram FW.

Statistical analysis was conducted with analysis of variance (ANOVA) and Student's t-test using the Statistical Package for the Social Sciences (SPSS) software (IBM SPSS Statistics, version 21.0, Armonk, USA).

Quantitative real-time PCR (qRT-PCR) analysis

qRT-PCR experiments were carried out with the same RNA samples for the transcriptome analysis on the ABI 7500 (Applied Biosystems, Carlsbad, USA). *X. sorbifolia Actin* (c24784. graph_c0) was used as an internal control. Specific primer pairs of selected genes were designed by Primer 5.0 with the primer sequences listed in S1 Table. Each reaction was performed in a 20-μL mixture using the TB Green® Premix Ex Taq™ II (TaKaRa, Dalian, China) according to the manufacturer's instructions. The relative expression levels of the genes were analyzed with ABI 7500 Software V2.3, and quantified using the $2^{-\Delta\Delta Ct}$ method, which represents the cycle threshold (CT) of the target gene relative to the reference *Actin* gene. Three independent biological replicates were used for qRT-PCR analysis.

Results

Malondialdehyde content, electrolyte leakage and antioxidant enzyme activity

MDA and EL levels are commonly used to assess the degree of membrane injury [49]. After low temperature stress, MDA content and EL value were significantly increased relative to the control, and they showed the same trend with the extension of the stress time (Fig 1A and 1B). MDA content and EL value increased rapidly within the first 4 h, then further increased slightly and reached peak level at 24 h, but subsequently decreased slowly until 48 h.

Compared to the control, lowering the temperature caused a general increase in the activities of all three enzymes in leaf tissue (Fig 1C–1E). The enzyme activities appeared a follow "rise to drop" tendency as time progressed. POD and CAT activity almost linearly increased during the first 12 h, and thereafter decreased sharply to the lowest level at 48 h, but it still higher than the control value. SOD activity initially increased slowly until 12 h, then rose rapidly and reached peak level at 24 h, but diminished sharply thereafter.

Transcriptome

The RNA-Seq analysis yielded approximately 92.53 Gb clean reads from 12 transcriptome libraries, on average 6.35 Gb for each library. Over 85% of the sequences in each library were mapped, indicating that the assembled transcriptome was available for differential expression analysis. The value of ≥Q30 was used to assess the quality of sequencing, and 93.65–94.38% of bases scoring Q30 for each library suggested that the RNA-Seq datasets are of high quality (Table 1). A total of 63,197 unigenes were obtained with an average length of 1,077 bp and N50 of 2,472 bp after assembly and data analysis, including 17,643 unigenes with lengths over 1 kb (S2 Table). The correlation heatmap analysis (S1 Fig) revealed that the 3 biological replicates showed high reproducibility for all treatments, and the gene expression data were closely related at each time point. In total 13,675, 13,544, 13,229, and 12,945 genes were expressed in the "Control", "LT_4h", "LT_12h", and "LT_24h", respectively, and a summary of the DEGs between samples at different time points is found in S2A Fig. The Venn diagram (S2B Fig) exhibits a total of 11,724 genes being expressed in all 5 groups, while 1,213 genes were specifically expressed in only 1 group ("Control", 549 genes; "LT_4h", 230 genes; "LT_12h", 142 genes; "LT_24h", 292 genes).
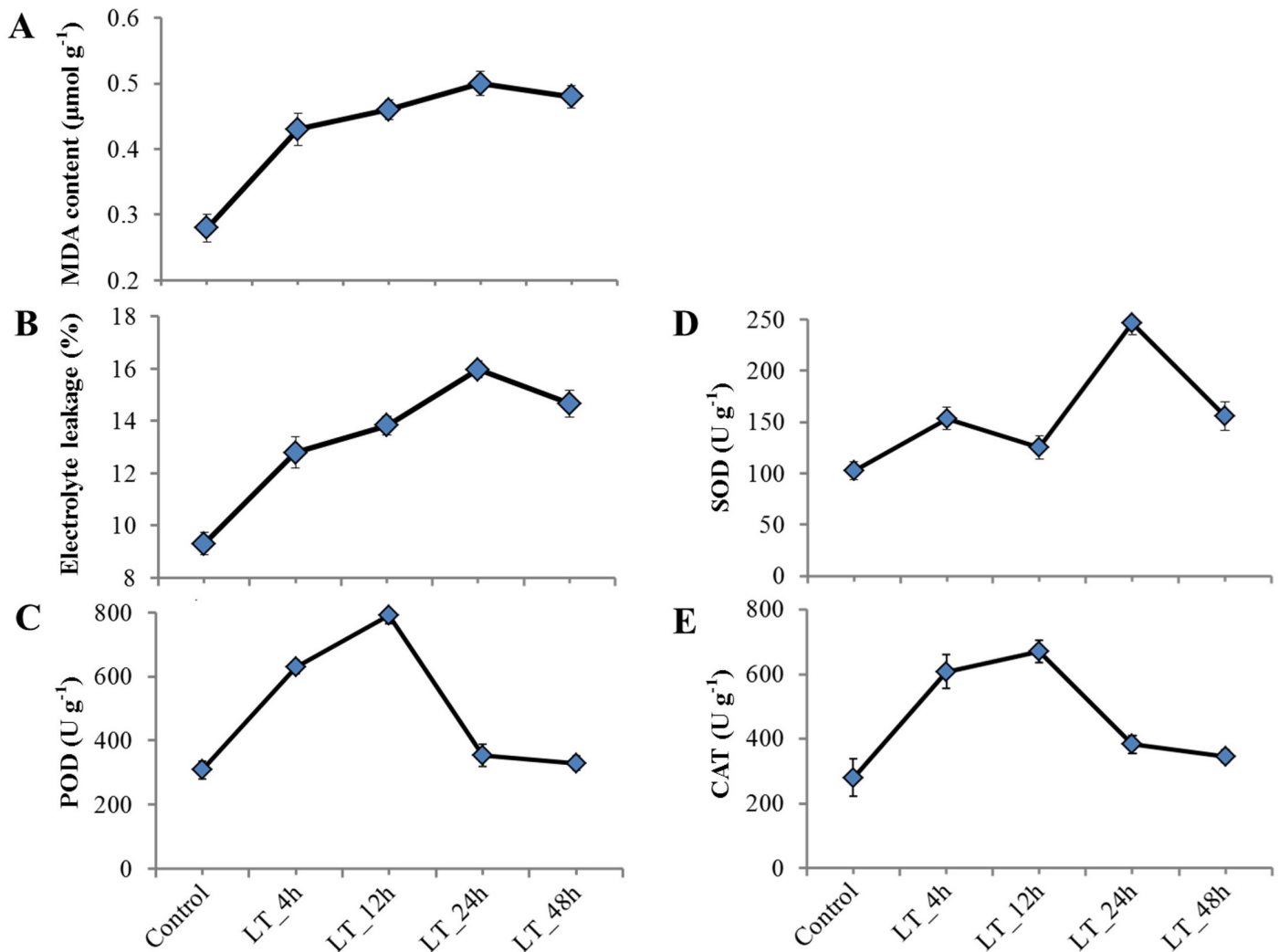
Fig 1. Changes in malondialdehyde content, electrolyte leakage and antioxidant enzyme activity in leaf tissues of *X. sorbifolia* under cold stress. (A) Malondialdehyde (MDA) content, (B) electrolyte leakage (EL), (C) Peroxidase (POD), (D) Superoxide Dismutase (SOD), and (E) Catalase (CAT). Error bars indicate means ± SD (n = 3).

Functional annotation

Each stress sample was compared with the control to identify DEGs. We identified 2,267 (1,281 up- and 986 downregulated) DEGs in the LT_4h sample, 4,062 (2,232 up- and 1,830 downregulated) DEGs in the LT_12h sample, and 7,904 (4,052 up- and 3,852 downregulated) DEGs in the LT_24h sample (Fig 2A), revealing that the number of upregulated DEGs was much higher than the number of downregulated DEGs. A total of 1,527 common DEGs, including 895 up- and 632 downregulated DEGs were identified and used for functional annotation (Fig 2B).

TF prediction

Based on all 81 families of TFs predicted from the *Arabidopsis* TF database [50], we detected 32 families with at least 1 gene matched to the DEG dataset. In total, 110 DEGs as TFs were identified in seedling leaves of *X. sorbifolia* in response to cold stress, including 76 up- and 34

Table 1. Overview of the transcriptome sequencing data.

Sample	Raw reads	Clean reads	Mapped reads	GC (%)	≥Q30 (%)
Control_1	7,171,112,530	24,041,522	20,842,522 (86.69%)	46.37	94.38
Control_2	8,368,100,334	28,077,693	24,279,069 (86.47%)	46.18	94.33
Control_3	9,418,103,704	31,593,500	27,360,921 (86.6%)	46.14	94.32
LT_4h_1	7,646,608,490	25,633,555	22,068,145 (86.09%)	47.17	94.20
LT_4h_2	8,899,831,612	29,829,113	25,835,520 (86.61%)	46.32	93.98
LT_4h_3	7,742,704,904	25,948,842	22,460,971 (86.56%)	46.25	93.94
LT_12h_1	6,896,939,568	23,136,097	19,954,286 (86.25%)	46.62	93.91
LT_12h_2	6,416,910,880	21,481,446	18,392,693 (85.62%)	46.06	93.90
LT_12h_3	8,452,995,722	28,341,540	24,367,088 (85.98%)	46.37	93.87
LT_24h_1	6,351,545,286	21,288,261	18,243,642 (85.7%)	46.03	93.82
LT_24h_2	7,906,165,170	26,511,245	22,833,381 (86.13%)	46.36	93.72
LT_24h_3	7,258,175,670	24,333,119	20,914,402 (85.95%)	46.33	93.65

downregulated TFs (Fig 3, S3 Table). Most of the TF families had more upregulated TFs than those that downregulated during cold stress compared with the control. In contrast, certain TFs belonging to the FAR and bHLH families showed more downregulation. In addition, WRKY, bHLH, ERF, MYB, and NAC families featured more active members, implying their important roles in the regulation of structural genes involved in cold response.

KEGG pathway classification

Under cold stress, the enrichment analysis of the DEGs based on the KEGG annotation showed that these genes mainly belonged to "metabolic pathways" (101 up- and 65 downregulated) and
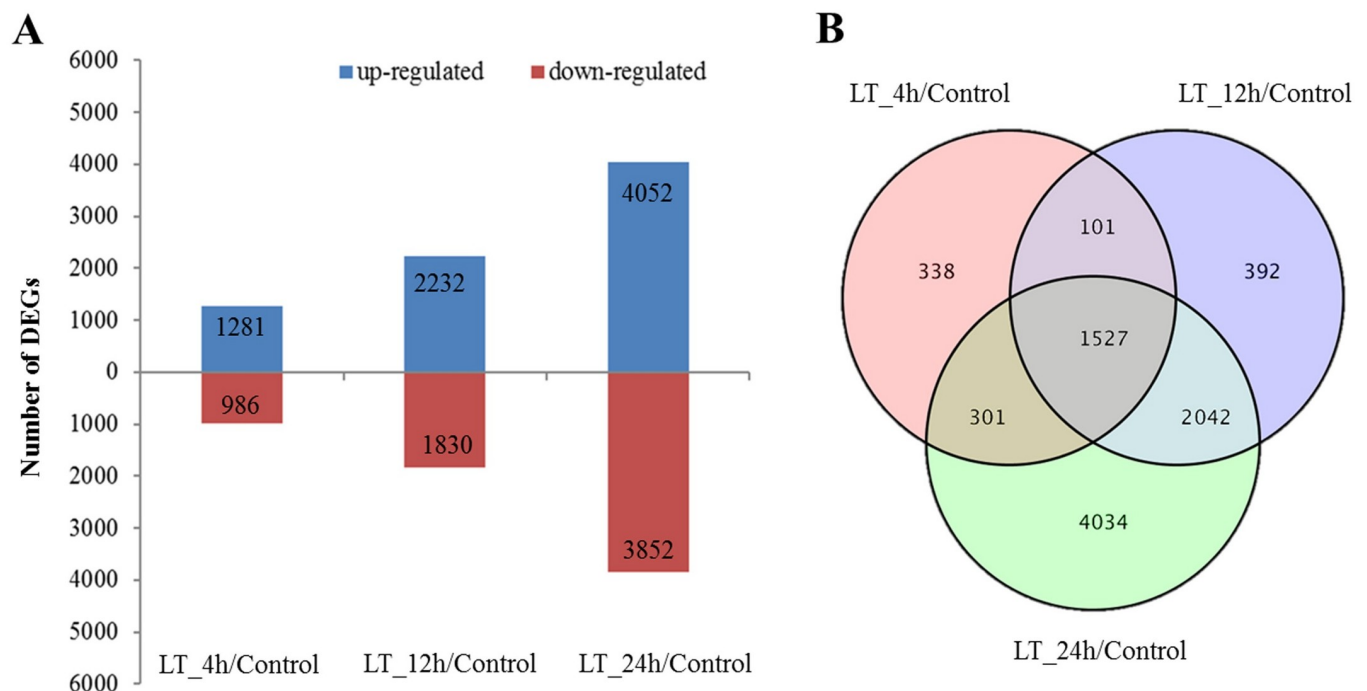

Fig 2. DEGs in the three pairwise comparisons of the control and stress treatments. (A) Bar chart showing the number of up- and downregulated genes in different comparisons. (B) Venn diagram showing the common and specific DEGs in different comparisons.
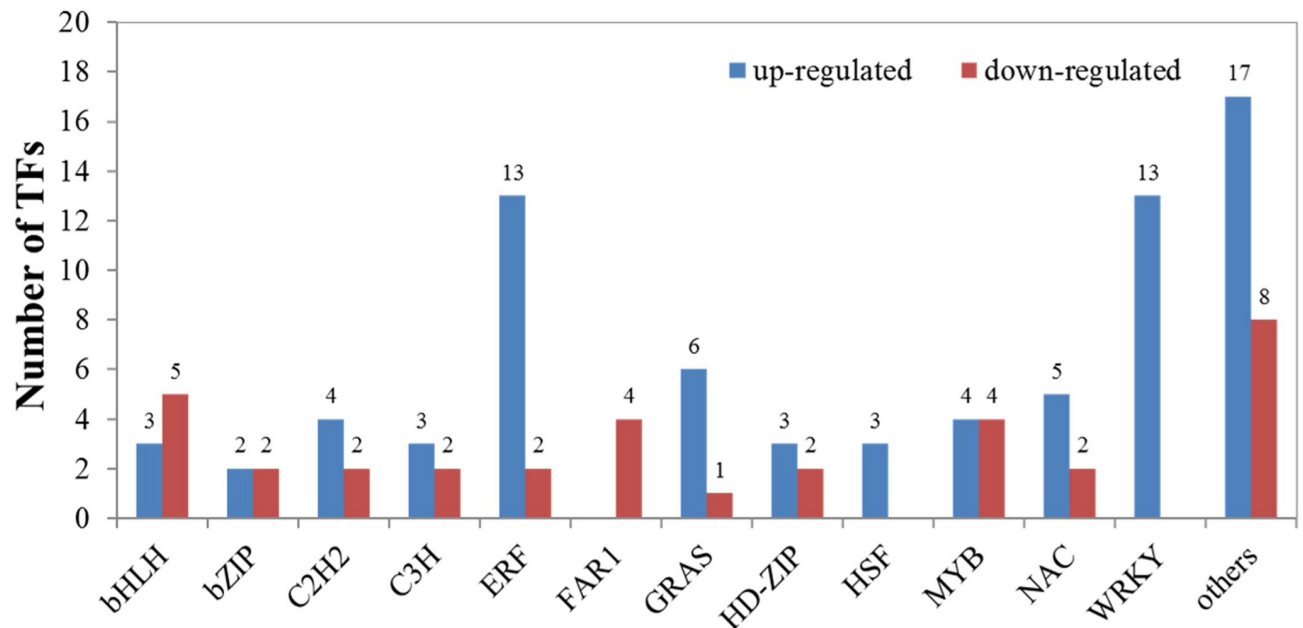
Fig 3. Distribution of the DEGs into different transcription factor families during cold stress. Blue and red colors indicate up- and downregulated transcripts, respectively.

"biosynthesis of secondary metabolites" (46 up- and 37 downregulated). In most pathways, the number of upregulated genes exceeded the downregulated genes. In particular, some pathways related to sugar metabolism and amino acid metabolism were enriched with DEGs, including amino acid metabolism, glycolysis/gluconeogenesis, starch and sucrose metabolism, galactose metabolism, fructose and mannose metabolism, and the citrate cycle (TCA cycle) (Fig 4). In addition, it is commonly accepted that the plant MAPK signaling pathway is highly conserved and plays a central role in plant abiotic stress responses [51]. Here, KEGG annotation detected that the MAPK signaling pathway was strongly affected by cold stress. A total of 12 DEGs were upregulated, whereas only 1 DEG was downregulated (S3 Fig), suggesting that the MAPK signaling pathway might be involved in regulating cold-stress response in *X. sorbifolia*. The upregulated genes were MEKK1 (c29943.graph_c1), WRKY33 (c36168.graph_c0), VIP1 (c35571.graph_c1), PP2C (c24440.graph_c0), MAPKKK17_18 (c26611.graph_c0), CaM4 (c25814.graph_c0), FLS2 (c30712.graph_c0), WRKY22 (c26048.graph_c0), WRKY29 (c22982.graph_c1), RTE1 (c33293.graph_c0), ERF1 (c20551.graph_c0), and RbohD (c29720.graph_c0).

GO annotation and classification

All the significantly enriched GO terms among the DEGs were assembled into a GO map (Fig 5) to help visualize the interactive networks, and network features were presented in S4 Table. A total of 991 (out of 1,527) DEGs were assigned to the 3 main GO functional categories, with 563 up- and 428 downregulated genes. Across the network of GO terms enriched from upregulated DEGs, 196 DEGs (34.81%) were assigned into the largest category, "cellular component", followed by "biological process" (186, 33.04%) and "molecular function" (181, 31.25%). A large number of DEGs were involved in some important GO terms that are known to be associated with cold tolerance in plants, such as "response to abiotic stimulus" (GO 9628, 8.88%), "response to endogenous stimulus" (GO 9719, 7.82%), and "response to stress" (GO 6950, 11.19%). For downregulated DEGs, the most frequent term for "biological process" was
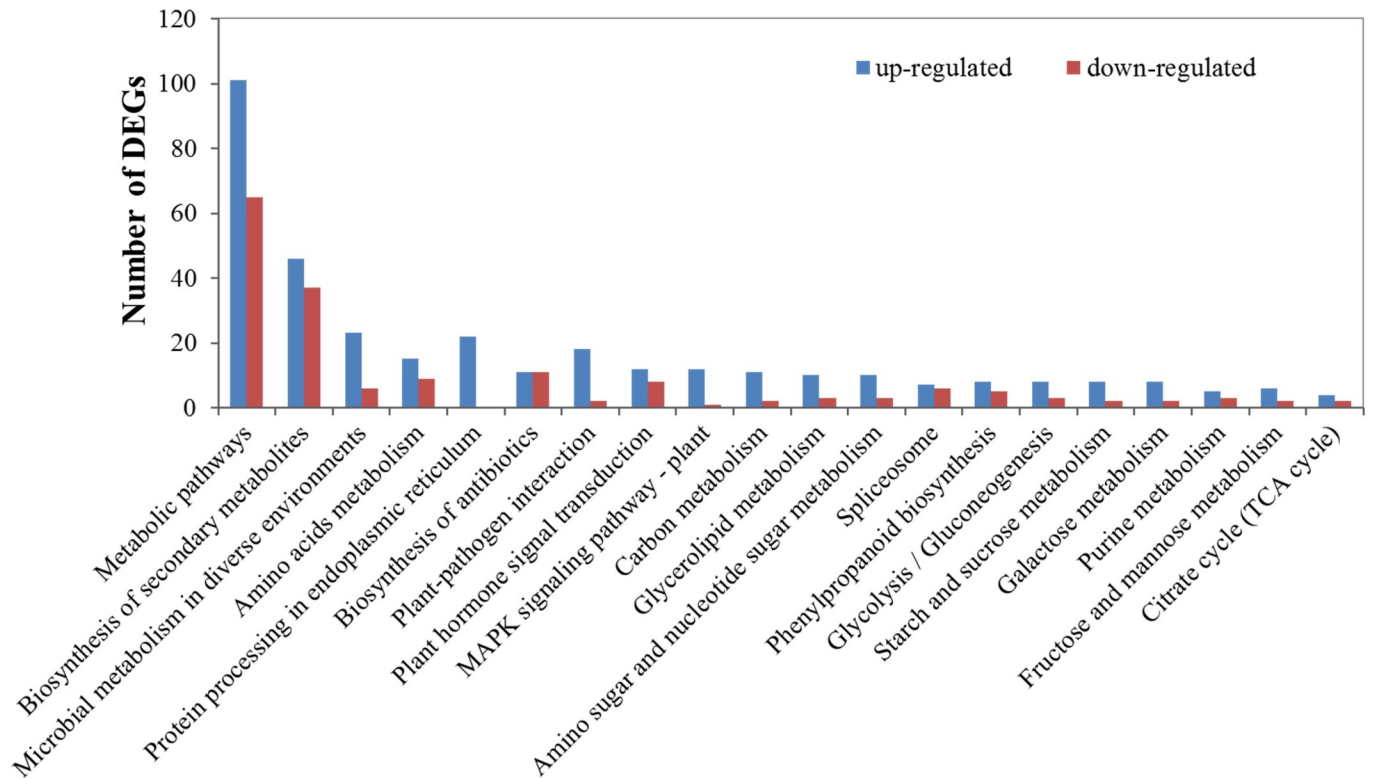
Fig 4. KEGG pathways enrichment of the DEGs during cold stress. Blue and red colors indicate up- and downregulated genes, respectively.

'cellular process' (GO 9987, 21.03%); within "cellular component", the most enriched term was related to 'membrane' (GO 16020, 13.08%); and the most enriched term within "molecular function" was 'catalytic activity' (GO 3824, 16.82%).

To further verify the reliability and accuracy of the RNA-Seq data, a total of 10 transcripts were selected for qRT-PCR analysis. The correlation analysis between qRT-PCR and RNA-Seq was measured by scatter plotting log2 (fold change), indicating that the expression patterns from qRT-PCR testing were highly consistent with the sequencing results (Pearson coefficient $r^2 = 0.88$; S4 Fig).

Metabolic profiling analysis

Leaf extracts from the control and cold treatments were subjected to metabolic profiling using a gas chromatograph-mass spectrometer. In total, 262 metabolites were identified and quantified in all samples, including a number of primary and secondary metabolites, such as amino acids, sugars, organic acids, lipids, alkaloids, and terpenoids. Compared to the control, 51 metabolites were significantly altered under cold stress, with 41 upregulated and 10 downregulated. To investigate the accumulation patterns of these significantly changed metabolites in response to cold stress, principal components analysis (PCA) and hierarchical clustering analysis (HCA) were carried out. PCA suggested that the first two principal components (PC1 and PC2), which were extracted and represented a clear separation for 6 samples from the control and treatment groups, explained 87.2% of the total variation (Fig 6A). HCA also revealed the responses to cold stress at the metabolite levels, and successfully distributed the tested samples into two major clusters (Fig 6B). Particularly, some measured metabolites were exclusively
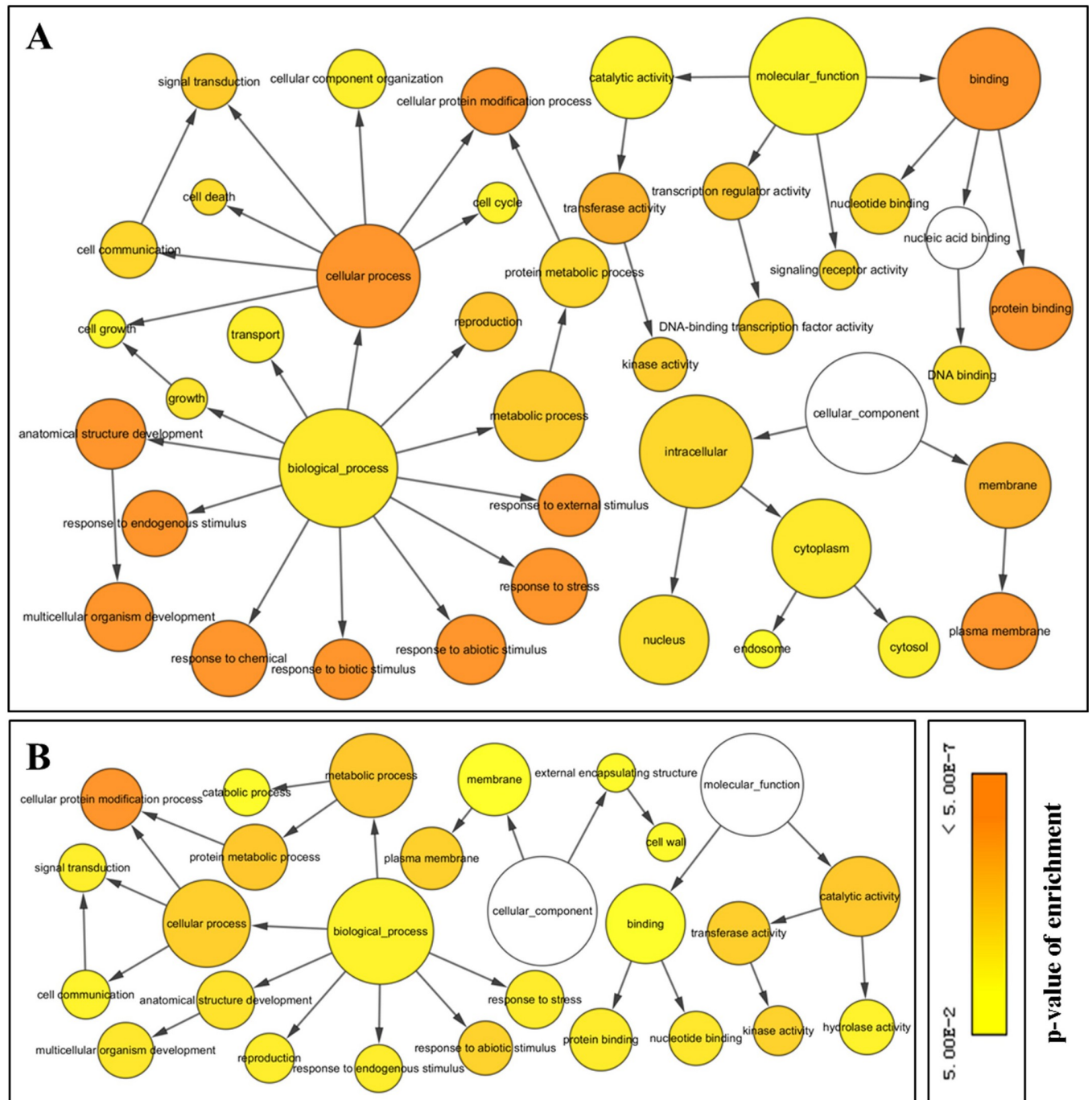
Fig 5. Networks of enriched GO terms in DEGs during cold stress. (A) Enriched GO terms from upregulated DEGs. (B) Enriched GO terms from downregulated DEGs. The lines represent the relationship between GO terms, with arrow from the higher ranking Go term pointing towards to the lower one. Circle size indicates the numbers of DEGs. Colors represent statistical significance.

https://doi.org/10.1371/journal.pone.0236588.g005

significantly increased by cold stress, such as a 6.7-fold rise in fructose, 4.1-fold in glucose, 7.1-fold in lactulose, 4.1-fold in proline, 17.8-fold in pyroglutamic acid, 2.3-fold in quinic acid, 2.3-fold in 3-hydroxybenzoic acid, 4.2-fold in sorbitol, 409.2-fold in xanthosine, and 10.8-fold in hydroquinone (S5 Table). Through metabolic pathway mapping, these significantly changed

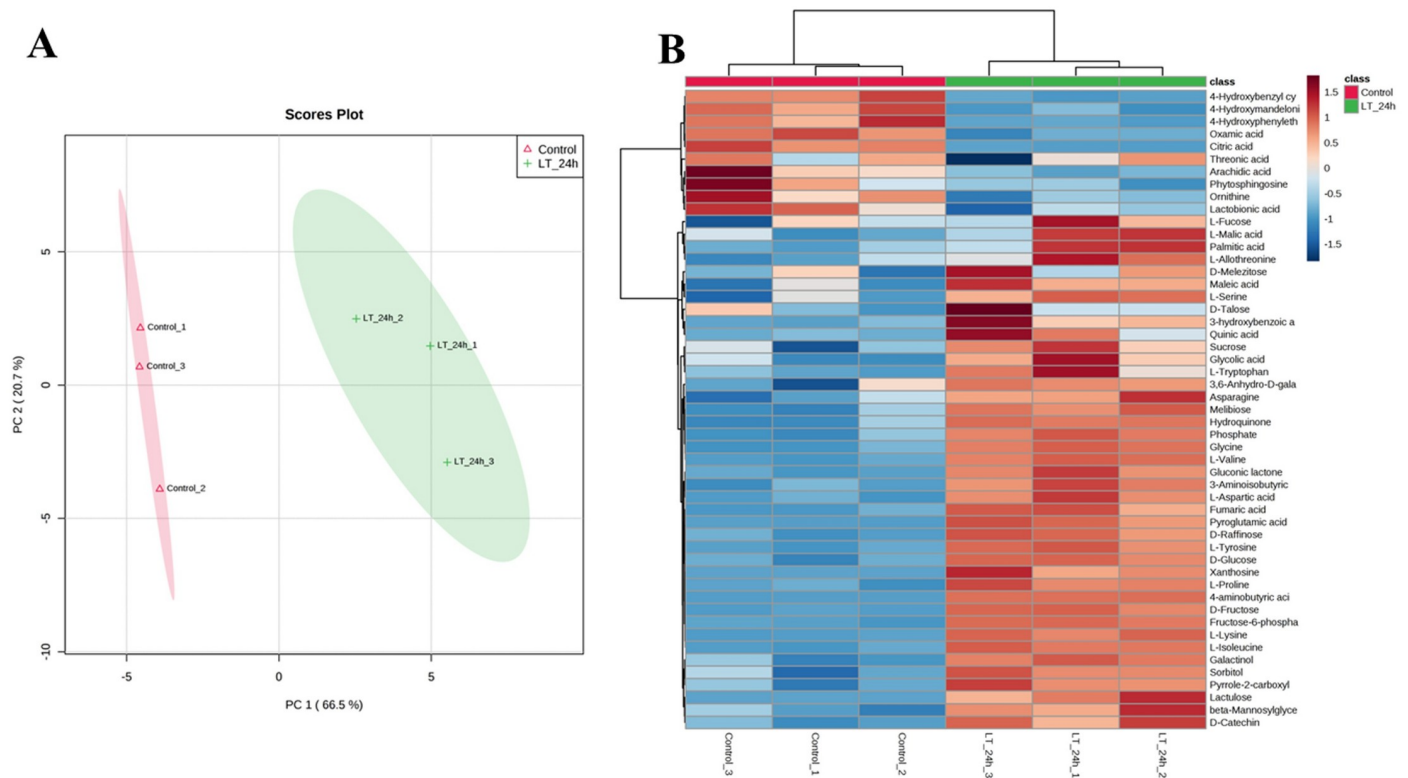**Fig 6. Metabolome analysis during cold stress in comparison with control.** (A) PCA score plot based on metabolome data. PC1 and PC2 are plotted on the x- and y-axes, respectively. (B) HCA of the fold changes in all significantly changed metabolites between control and treatments.

metabolites were mainly annotated with amino acid metabolism, carbohydrate metabolism, aminoacyl-tRNA biosynthesis, and the TCA cycle, implying that these metabolic pathways play important roles in stress signaling and responses in *X. sorbifolia* (S5 Fig).

Conjoint analysis of gene expression and metabolite levels involved in key biological pathways

In plants, sugars and amino acids as osmotic substances are crucial regulatory elements during stress response. Interestingly, KEGG pathways involved in amino acid metabolism and sugar metabolism were enriched in both metabolite levels and gene expression under cold stress. Schematic diagrams of amino acid and sugar biosynthetic pathways of *X. sorbifolia* are presented in Fig 7A. The levels of most amino acids and sugars were significantly increased, suggesting that the accumulation of amino acids and sugars are important for the cold-stress response. Fig 7B shows the expression patterns of genes involved in the pathways at different time points. Within the pathways, cold stress resulted in the strong accumulation of fructose, glucose, raffinose, melibiose, galactinol, valine, glycine, lysine, isoleucine, tryptophan, serine, aspartate, proline, asparagine, and tyrosine. Most of the genes involved in the biosynthesis of these metabolites were upregulated, while there was a trend of downregulation among some genes of these pathways. The genes encoding beta-fructofuranosidase, mannose isomerase, raffinose synthase, and hexokinase (involved in sugar metabolism) were upregulated by cold stress; however, two genes encoding alpha-galactosidase and aldehyde reductase were downregulated. The gene encoding pyrroline-5-carboxylate synthase (P5CS, catabolizes the synthesis of proline) was upregulated; in contrast, one gene encoding proline dehydrogenase
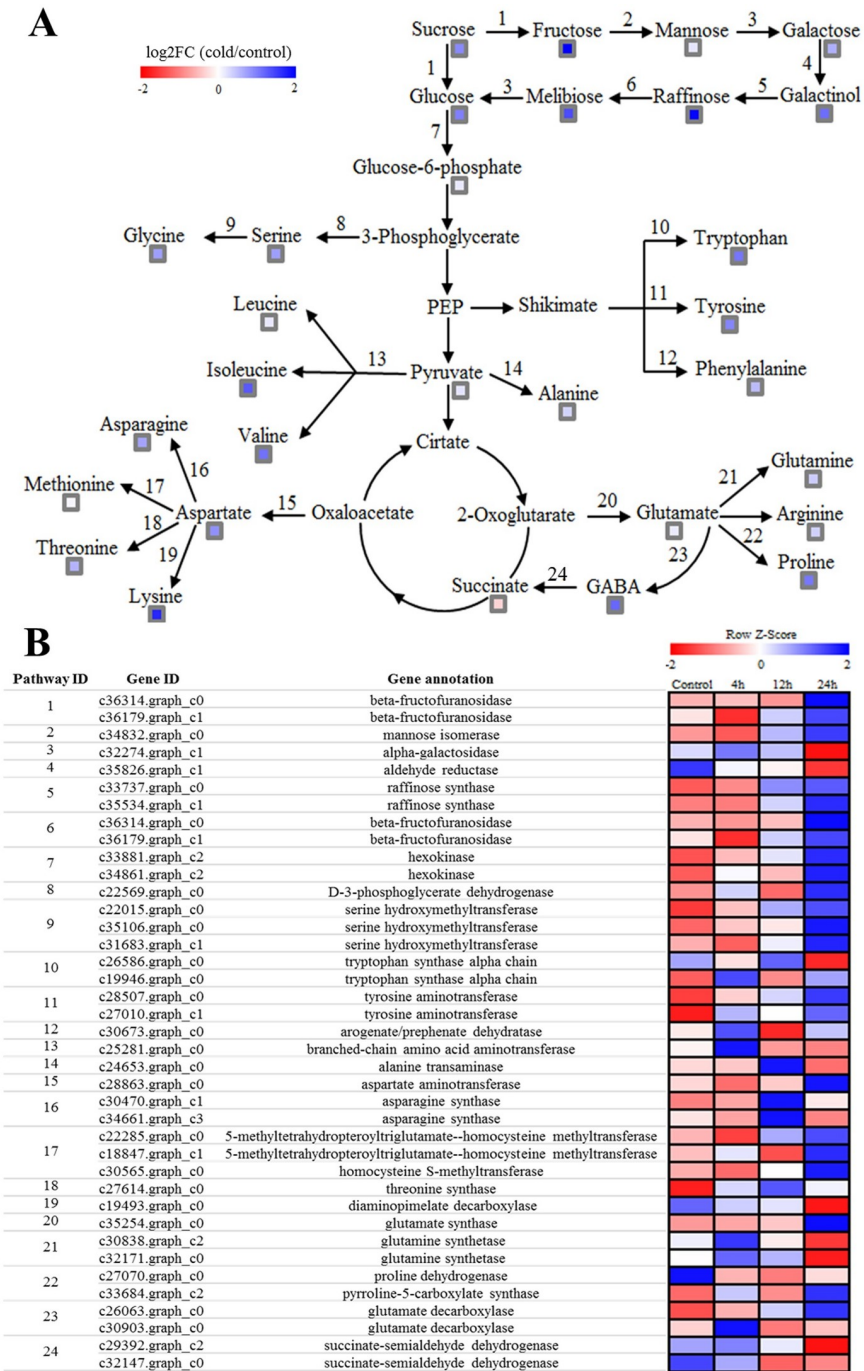
Fig 7. Overview of sugar and amino acid metabolic pathways during cold stress. (A) Changes of the metabolites associated with the pathways at 24 h after cold stress. (B) Expression patterns of the genes involved in metabolic pathways at different time points.

https://doi.org/10.1371/journal.pone.0236588.g007

(catabolizes the degradation of proline) was downregulated. This was consistent with the elevated proline levels under cold stress. The lysine levels rose despite the downregulation of a related gene. The levels of other amino acids (such as serine, glycine, isoleucine, tryptophan) were increased within the amino acid metabolic pathways, and the expression levels of related

genes involved in these pathways were upregulated at almost all time points. Two genes encoding succinate-semialdehyde dehydrogenase were downregulated, which was associated with reduced succinate levels under cold stress.

Discussion

Signaling transduction and regulation during cold stress

LT is initially recognized by the plasma membrane either based on alterations in membrane fluidity or with the aid of sensory proteins, such as Ca^{2+}-permeable channels [52]. The membrane permeability of Ca^{2+} receptors was enhanced to allow more Ca^{2+} entry into the plasma after plants received cold signals, resulting in rapid accumulation of Ca^{2+} in the cytosol. Ca^{2+} is an important second messenger that plays a key role in the response to cold stress [53]. For instance, cold stress can cause an immediate rise in cytosolic free-Ca^{2+} concentration and activate Ca^{2+}-permeable channels in *Arabidopsis* mesophyll cells [54]. Ca^{2+} sensors perceive intracellular changes in Ca^{2+} levels via phosphorylation and then transduce the signals in order to switch on downstream signaling processes for expression of cold-specific genes, which help in the adaptation of plants to cold stress [55]. The main intracellular Ca^{2+} sensors in plants are calmodulin (CaM), calcium-dependent protein kinases (CDPKs), calcineurin B-like proteins (CBLs), and their interacting protein kinases (CIPKs). In the present study, 12 DEGs were involved in the Ca^{2+} signaling pathway, of which 8 genes were upregulated and 4 genes were downregulated (S6A Fig). These upregulated genes contained 2 CaMs (c25814.graph_c0 and c29478.graph_c0), 2 CDPKs (c28536.graph_c1 and c32077.graph_c0), 2 CBLs (c35219.graph_c0 and c34566.graph_c3), and 2 CIPKs (c23992.graph_c0 and c28195.graph_c0), suggesting that they are associated with Ca^{2+} signaling and promote an increased intracellular Ca^{2+} concentration to activate various transcriptional cascades.

Besides calcium influx, abiotic stress can also cause the accumulation of ROS in the cytosol [18]. ROS has a signaling function that mediates defense gene activation by redox-sensitive transcription factors or via interaction with other signaling components, such as the MAPK cascade [56]. The MAPK cascade is a common signal transduction module that connects signals from receptors/sensors to nuclear and cellular responses [57, 58]. A total of 13 DEGs were involved in the plant-MAPK signaling pathway according to KEGG pathway annotation, and almost all DEGs were upregulated by cold stress (S6B Fig). It has been reported for *Arabidopsis* that the MAPKKK (MAP kinase kinase)-MAPKK (MAP kinase kinase)-MAPK cascade could be activated by ROS to enhance the cold resistance of plants [59]. Cold stress may also activate the MAPK cascade in *X. sorbifolia* to regulate gene expression, and MEKK1 and MAPKKK17_18 as cascade members were upregulated by cold stress. The MAPK cascade acts downstream of FLS2 to activate gene expression in *Arabidopsis* [60], and FLS2 was also upregulated by cold stress in *X. sorbifolia*. PP2C is a regulator of various signal transduction pathways that participate in stress response [61]. Evidences have indicated that PP2C controls the activation level of MAPK signaling [62], and it was upregulated by cold stress in our findings. The upregulation of ERF and CaM4 in the MAPK signaling pathway has been proposed as a secondary signal receptor of ethylene and Ca^{2+}, respectively.

Changes in ROS-scavenging system during cold stress

Intracellular ROS are thought to play a decisive role in regulating signal transduction events, but stress can cause ROS accumulation [63]. Excessive ROS enhance membrane lipid peroxidation (LPO) and disrupts membrane fluidity, resulting in electrolyte leakage (EL) [64]. Malondialdehyde (MDA) is also a peroxide lipid derivative, and its production can exacerbate membrane damage [65]. Here, Low-temperature treatment increased MDA concent and EL

value in *X. sorbifolia*, indicating that cold stress caused probably the disruption of the plasma membrane. However, ROS homeostasis depends largely on ROS-scavenging systems under abiotic stress conditions [49, 66]. In the present study, we found a rise in the activity of ROS-scavenging enzymes (including SOD, CAT, and POD), suggesting a positive response when removing ROS generated by cold stress in *X. sorbifolia*. SOD is a scavenger of peroxide anions, which disproportionates the anions into H_2O_2 and O_2 [63]. Meanwhile, POD and CAT can catalyze the conversion of H_2O_2 into oxygen and water [67]. The increase in SOD activity was lower than that of POD and CAT, potentially owing to POD and CAT having higher capacity for the decomposition of H_2O_2 generated by SOD. In addition, certain cold-responsive genes encoding anti-oxidative enzymes involved in the ROS-scavenging system, such as peroxidase (c32290.graph_c1 and else) and glutathione S-transferase (c35048.graph_c4), were strongly upregulated under cold stress, implying their significance in the ROS-scavenging system. Overall, the cold-induced enhancement of enzyme activity and gene expression might improve the ROS detoxification ability of *X. sorbifolia* against the detrimental effects of oxidative stress.

Osmoprotectants metabolism during cold stress

Cold stress can induce osmotic stress in plant cells. Many plants maintain a stable osmotic pressure via the biosynthesis of osmoprotectants in the cold-stress response. Osmoprotectants are involved in the regulation of cellular water relations and reduce cellular dehydration [4]; moreover, they are non-toxic and accumulate at significant levels without upsetting plant metabolism [68]. In our study, strong cold-induced accumulation was observed in most of the amino acids, sugars, and sugar alcohols (S5 Table), while many of them can function as osmolytes in the cytoplasm under cold stress in plants [4]. Previous reports showed that various stress-responsive metabolites of plants were synthesized from amino acid metabolic pathways, suggesting that amino acid metabolism plays an important role in response to stress in plants [69]. For instance, proline accumulation in many plants is a common physiological response to abiotic stresses, such as LT, drought, and high salinity [70–72]. Proline is known to stabilize proteins, membranes, and subcellular structures, and protect cellular functions by scavenging ROS. The proline content was increased by cold stress and the important proline synthesis gene (P5CS, c33684.graph_c2) was upregulated, while the proline degradation gene (proline dehydrogenase, c27070.graph_c0) was downregulated (Fig 7B). Therefore, proline accumulation in *X. sorbifolia* under cold stress was based on co-regulation of P5C5 and proline dehydrogenase. Meanwhile, we detected the upregulation of several genes involved in amino acid metabolism and sugar metabolism, which was also consistent with the accumulation of special cold-responsive metabolites. In short, the changes observed at the transcriptomic and metabolic levels strongly revealed that accumulation of these cold-responsive metabolites by synthesis or metabolism pathways might contribute to cold-stress defense and thereby minimize cold damage.

Transcription factors involved in response to cold stress

Many studies have shown that TFs are involved in transcriptional networks responding to abiotic stress in plants [73–75]. Consistent with findings in other plants, our transcriptomic data showed that most of the differentially expressed TFs belonged to the ERF, WRKY, NAC, bHLH, and MYB TF families, indicating the multiplicity and complexity of the regulatory pathways in response to cold stress [8, 76]. The ERF TF family was the largest class responding to cold stresses, with 13 upregulated and 2 downregulated DEGs. In particular, CBF/DREB from the ERF superfamily has been reported to play a vital role in regulating cold-responsive gene changes in many plants [77–79]. This was strengthened by the observation that a CBF TF

(c28392.graph_c0) was significantly upregulated (132-fold), which played a direct role in activating the expression of downstream genes like COR. Currently, growing evidence has demonstrated that WRKY TFs are widely implicated in plant-stress responses [80, 81]. Notably, 13 WRKY family members in *X. sorbifolia* were all upregulated. Therefore, the overrepresentation of this TF family may indicate their importance in improving the resistance to cold response in *X. sorbifolia*. The plant-specific NAC TF family is involved in the regulation of multiple pathways, including plant development, hormone signaling, and stress response. RD26, which encodes a NAC TF, could remarkably enhance resistance to stress responses in *Arabidopsis* [82]. We found 8 genes encoding NAC TFs, and almost all were upregulated. These results emphasize that TFs play vital parts in enhancing cold resistance of *X. sorbifolia*. In addition, some of the MYB and bHLH TF family members were downregulated. MYB and bHLH TFs have also been reported to be involved in stress responses [83, 84], and they often interact with each other to control transcription [85]. Therefore, we deduced that these partner factors may be required in response to different cold conditions.

Conclusions

In summary, cold stress caused significant changes in physiological, transcriptomic, and metabolomic levels in the leaves of *X. sorbifolia*. Based on the transcriptomic and metabolomics datasets, we successfully identified a number of candidate genes and metabolites that participate in crucial biological pathways during the cold-stress response. This was the first study to investigate the combined metabolomic and transcriptomic features of *X. sorbifolia* under cold stress, which reveals a complex regulation network and series of signaling mechanisms. These results provide useful insights into the tolerance mechanism of *X. sorbifolia* responding to cold stress.

Supporting information

S1 Fig. Pearson correlation analysis of sample replicates.
(TIF)

S2 Fig. Summary of active genes at different cold stress time points (A), and Venn diagrams showing overlap in numbers of expressed genes from control and treated samples (B).
(TIF)

S3 Fig. Plant-MAPK signaling pathway (Ko04016) map. Blue boxes indicated the up-regulated DEGs in leaf tissues of *X. sorbifolia* under cold stress.
(TIF)

S4 Fig. Correlation analysis between qRT-PCR and RNA-Seq data based on log2 (fold change) of 10 selected genes.
(TIF)

S5 Fig. Metabolic pathways annotation of 51 significantly changed metabolites.
(TIF)

S6 Fig. Heatmap of DEGs involved in Ca^{2+} and MAPK signaling pathway in the three pairwise comparisons of control and stress treatments.
(TIF)

S1 Table. Primers used in qRT-PCR analysis.
(XLS)

S2 Table. Statistics of the unigene assembly results.
(XLS)

S3 Table. DEGs encoding transcription factor families.
(XLS)

S4 Table. Summary of gene ontology (GO) enrichment of DEGs in *X. sorbifolia* in response to cold stress.
(XLS)

S5 Table. The detail information of differentially changed metabolites in *X. sorbifolia* under cold stress.
(XLS)

Acknowledgments

Author Contributions

Conceptualization: Jinping Guo.

Data curation: Juan Wang, Yunxiang Zhang, Xingrong Yan.

Formal analysis: Juan Wang.

Investigation: Xingrong Yan.

Methodology: Yunxiang Zhang.

Project administration: Jinping Guo.

Resources: Yunxiang Zhang, Xingrong Yan.

Writing – original draft: Juan Wang.

Writing – review & editing: Juan Wang, Jinping Guo.

References

1. Sanghera GS, Wani SH, Hussain W, Singh N. Engineering cold stress tolerance in crop plants. Current genomics. 2011; 12(1):30. https://doi.org/10.2174/138920211794520178 PMID: 21886453

2. Khan MS, Khan MA, Ahmad D. Assessing utilization and environmental risks of important genes in plant abiotic stress tolerance. Frontiers in plant science. 2016; 7:792. https://doi.org/10.3389/fpls.2016.00792 PMID: 27446095

3. Ali A, Maggio A, Bressan RA, Yun DJ. Role and functional differences of HKT1-type transporters in plants under salt stress. International journal of molecular sciences. 2019; 20(5):1059. https://doi.org/10.3390/ijms20051059 PMID: 30823627

4. Yadav SK. Cold stress tolerance mechanisms in plants. A review. Agronomy for Sustainable Development. 2010; 30(3):515–527. https://doi.org/10.1051/agro/2009050

5. de Zelicourt A, Colcombet J, Hirt H. The role of MAPK modules and ABA during abiotic stress signaling. Trends in plant science. 2016; 21(8):677–685. https://doi.org/10.1016/j.tplants.2016.04.004 PMID: 27143288

6. Bailey-Serres J, Mittler R. The roles of reactive oxygen species in plant cells. Plant Physiology. 2006; 141(2):311. https://doi.org/10.1104/pp.104.900191 PMID: 16760480

7. Verslues PE, Agarwal M, Katiyar-Agarwal S, Zhu J, Zhu JK. Methods and concepts in quantifying resistance to drought, salt and freezing, abiotic stresses that affect plant water status. The Plant Journal. 2006; 45(4):523–539. https://doi.org/10.1111/j.1365-313X.2005.02593.x PMID: 16441347

8. Li YY, Wang XW, Ban QY, Zhu XX, Jiang CJ, Wei CL, et al. Comparative transcriptomic analysis reveals gene expression associated with cold adaptation in the tea plant *Camellia sinensis*. BMC genomics. 2019; 20(1):624. https://doi.org/10.1186/s12864-019-5988-3 PMID: 31366321

9. Theocharis A, Clément C, Barka EA. Physiological and molecular changes in plants grown at low temperatures. Planta. 2012; 235(6):1091–1105. https://doi.org/10.1007/s00425-012-1641-y PMID: 22526498

10. Wu ZG, Jiang W, Chen SL, Mantri N, Tao ZM, Jiang CX. Insights from the cold transcriptome and metabolome of *Dendrobium officinale*: global reprogramming of metabolic and gene regulation networks during cold acclimation. Frontiers in plant science. 2016; 7:1653. https://doi.org/10.3389/fpls.2016.01653 PMID: 27877182

11. Medina J, Catalá R, Salinas J. The CBFs: three *Arabidopsis* transcription factors to cold acclimate. Plant Science. 2011; 180(1):3–11. https://doi.org/10.1016/j.plantsci.2010.06.019 PMID: 21421341

12. Cook D, Fowler S, Fiehn O, Thomashow MF. A prominent role for the CBF cold response pathway in configuring the low-temperature metabolome of *Arabidopsis*. Proceedings of the National Academy of Sciences. 2004; 101(42):15243–15248.

13. Klepikova AV, Kulakovskiy IV, Kasianov AS, Logacheva MD, Penin AA. An update to database TraVA: organ-specific cold stress response in *Arabidopsis thaliana*. BMC plant biology. 2019; 19(1):49. https://doi.org/10.1186/s12870-019-1636-y PMID: 30813912

14. Jeon J, Kim J. Cold stress signaling networks in *Arabidopsis*. Journal of Plant Biology. 2013; 56(2):69–76. https://doi.org/10.1007/s12374-013-0903-y

15. Di Fenza M, Hogg B, Grant J, Barth S. Transcriptomic response of maize primary roots to low temperatures at seedling emergence. PeerJ. 2017; 5:e2839. https://doi.org/10.7717/peerj.2839 PMID: 28168096

16. Sobkowiak A, Jończyk M, Jarochowska E, Biecek P, Trzcinska-Danielewicz J, Leipner J, et al. Genome-wide transcriptomic analysis of response to low temperature reveals candidate genes determining divergent cold-sensitivity of maize inbred lines. Plant molecular biology. 2014; 85(3):317–331. https://doi.org/10.1007/s11103-014-0187-8 PMID: 24623520

17. Shen CX, Li D, He RH, Fang Z, Xia YM, Gao J, et al. Comparative transcriptome analysis of RNA-seq data for cold-tolerant and cold-sensitive rice genotypes under cold stress. Journal of Plant Biology. 2014; 57(6):337–348. https://doi.org/10.1007/s12374-014-0183-1

18. da Maia LC, Cadore PR, Benitez LC, Danielowski R, Braga EJ, Fagundes PR, et al. Transcriptome profiling of rice seedlings under cold stress. Functional Plant Biology. 2017; 44(4):419–429. https://doi.org/10.1071/FP16239 PMID: 32480575

19. Xu H, Gao Y, Wang JB. Transcriptomic analysis of rice (*Oryza sativa*) developing embryos using the RNA-Seq technique. PLoS ONE. 2012; 7(2):e30646. https://doi.org/10.1371/journal.pone.0030646 PMID: 22347394

20. da Silva FG, Iandolino A, Al-Kayal F, Bohlmann MC, Cushman MA, Lim H, et al. Characterizing the grape transcriptome. Analysis of expressed sequence tags from multiple Vitis species and development of a compendium of gene expression during berry development. Plant physiology. 2005; 139(2):574–597. https://doi.org/10.1104/pp.105.065748 PMID: 16219919

21. Jiao Y, Shen ZJ, Yan J. Transcriptome analysis of peach [*Prunus persica* (L.) Batsch] stigma in response to low-temperature stress with digital gene expression profiling. Journal of Plant Biochemistry and Biotechnology. 2017; 26(2):141–148. https://doi.org/10.1007/s13562-016-0374-6

22. Arbona V, Manzi M, Ollas CD, Gómez-Cadenas A. Metabolomics as a tool to investigate abiotic stress tolerance in plants. International journal of molecular sciences. 2013; 14(3):4885–4911. https://doi.org/10.3390/ijms14034885 PMID: 23455464

23. Sun CX, Gao XX, Li MQ, Fu JQ, Zhang YL. Plastic responses in the metabolome and functional traits of maize plants to temperature variations. Plant biology. 2016; 18(2):249–261. https://doi.org/10.1111/plb.12378 PMID: 26280133

24. Shiryaeva L, Antti H, Schröder WP, Strimbeck R, Shiriaev AS. Pair-wise multicomparison and OPLS analyses of cold-acclimation phases in Siberian spruce. Metabolomics. 2012; 8(1):123–130. https://doi.org/10.1007/s11306-011-0304-5 PMID: 22593724

25. Perotti VE, Moreno AS, Trípodi KE, Meier G, Bello F, Cocco M, et al. Proteomic and metabolomic profiling of Valencia orange fruit after natural frost exposure. Physiologia plantarum. 2015; 153(3):337–354. https://doi.org/10.1111/ppl.12259 PMID: 25132553

26. Pagter M, Alpers J, Erban A, Kopka J, Zuther E, Hincha DK. Rapid transcriptional and metabolic regulation of the deacclimation process in cold acclimated *Arabidopsis thaliana*. BMC genomics. 2017; 18(1):731. https://doi.org/10.1186/s12864-017-4126-3 PMID: 28915789

27. Guo HH, Wang TT, Li QQ, Zhao N, Zhang Y, Liu D, et al. Two novel diacylglycerol acyltransferase genes from *Xanthoceras sorbifolia* are responsible for its seed oil content. Gene. 2013; 527(1):266–274. https://doi.org/10.1016/j.gene.2013.05.076 PMID: 23769928

28. Ruan CJ, Yan R, Wang BX, Mopper S, Guan WK, Zhang J. The importance of yellow horn (*Xantho-ceras sorbifolia*) for restoration of arid habitats and production of bioactive seed oils. Ecological engineering. 2017; 99:504–512. https://doi.org/10.1016/j.ecoleng.2016.11.073

29. Yao ZY, Qi JH, Yin LM. Biodiesel production from *Xanthoceras sorbifolia* in China: opportunities and challenges. Renewable and Sustainable Energy Reviews. 2013; 24:57–65. https://doi.org/10.1016/j.rser.2013.03.047

30. Chen S, Zhang X. Characterization of the complete chloroplast genome of *Xanthoceras sorbifolium*, an endangered oil tree. Conservation Genetics Resources. 2017; 9(4):595–598. https://doi.org/10.1007/s12686-017-0732-2

31. Liang Q, Li H, Li S, Yuan F, Sun J, Duan Q, et al. The genome assembly and annotation of yellowhorn (*Xanthoceras sorbifolium* Bunge). Gigascience. 2019; 8(6):1–15. https://doi.org/10.1093/gigascience/giz071 PMID: 31241155

32. Bi Q, Zhao Y, Du W, Lu Y, Gui L, Zheng Z, et al. Pseudomolecule-level assembly of the Chinese oil tree yellowhorn (*Xanthoceras sorbifolium*) genome. Gigascience. 2019; 8(6):1–11. https://doi.org/10.1093/gigascience/giz070 PMID: 31241154

33. Wang L, Ruan C, Liu L, Du W, Bao A. Comparative RNA-Seq analysis of high- and low-oil yellow horn during embryonic development. International Journal of Molecular Sciences. 2018; 19(10):3071. https://doi.org/10.3390/ijms19103071 PMID: 30297676

34. Liu Y, Huang Z, Ao Y, Li W, Zhang Z. Transcriptome analysis of yellow horn (*Xanthoceras sorbifolia* Bunge): a potential oil-rich seed tree for biodiesel in China. PLoS ONE. 2013; 8(9):e74441. https://doi.org/10.1371/journal.pone.0074441 PMID: 24040247

35. Zhou Q, Zheng Y. Comparative De Novo transcriptome analysis of fertilized ovules in *Xanthoceras sorbifolium* uncovered a pool of genes expressed specifically or preferentially in the selfed ovule that are potentially involved in late-acting self-incompatibility. PLoS ONE. 2015; 10(10):e0140507. https://doi.org/10.1371/journal.pone.0140507 PMID: 26485030

36. Lang Y, Liu Z, Zheng Z. Investigation of yellow horn (*Xanthoceras sorbifolia* Bunge) transcriptome in response to different abiotic stresses: a comparative RNA-Seq study. RSC Advances. 2020; 10 (11):6512–6519. https://doi.org/10.1039/c9ra09535g

37. Kanehisa M, Goto S, Kawashima S, Okuno Y, Hattori M. The KEGG resource for deciphering the genome. Nucleic acids research. 2004; 32(suppl_1):D277–D280. https://doi.org/10.1093/nar/gkh063 PMID: 14681412

38. Ashburner M, Ball CA, Blake JA, Botstein D, Butler H, Cherry JM, et al. Gene ontology: tool for the unification of biology. Nature genetics. 2000; 25(1):25–29. https://doi.org/10.1038/75556 PMID: 10802651

39. Tatusov RL, Galperin MY, Natale DA, Koonin EV. The COG database: a tool for genome-scale analysis of protein functions and evolution. Nucleic acids research. 2000; 28(1):33–36. https://doi.org/10.1093/nar/28.1.33 PMID: 10592175

40. Huerta-Cepas J, Szklarczyk D, Forslund K, Cook H, Heller D, Walter MC, et al. eggNOG 4.5: a hierarchical orthology framework with improved functional annotations for eukaryotic, prokaryotic and viral sequences. Nucleic acids research. 2016; 44(D1):D286–D293. https://doi.org/10.1093/nar/gkv1248 PMID: 26582926

41. Apweiler R, Bairoch A, Wu CH, Barker WC, Boeckmann B, Ferro S, et al. UniProt: the universal protein knowledgebase. Nucleic acids research. 2004; 32(suppl_1):D115–D119. https://doi.org/10.1093/nar/gkh131 PMID: 14681372

42. Deng YY, Li JQ, Wu SF, Zhu YP, He FC. Integrated nr database in protein annotation system and its localization. Computer Engineering. 2006; 32(5):71–72.

43. Koonin EV, Fedorova ND, Jackson JD, Jacobs AR, Krylov DM, Makarova KS, et al. A comprehensive evolutionary classification of proteins encoded in complete eukaryotic genomes. Genome biology. 2004; 5(2):R7. https://doi.org/10.1186/gb-2004-5-2-r7 PMID: 14759257

44. Altschul SF, Madden TL, Schäffer AA, Zhang J, Zhang Z, Miller W, et al. Gapped BLAST and PSI-BLAST: a new generation of protein database search programs. Nucleic acids research. 1997; 25 (17):3389–3402. https://doi.org/10.1093/nar/25.17.3389 PMID: 9254694

45. Mortazavi A, Williams BA, McCue K, Schaeffer L, Wold B. Mapping and quantifying mammalian transcriptomes by RNA-Seq. Nature methods. 2008; 5(7):621. https://doi.org/10.1038/nmeth.1226 PMID: 18516045

46. Li PC, Cao W, Fang HM, Xu SH, Yin SY, Zhang YY, et al. Transcriptomic profiling of the maize (*Zea mays* L.) leaf response to abiotic stresses at the seedling stage. Frontiers in plant science. 2017; 8:290. https://doi.org/10.3389/fpls.2017.00290 PMID: 28298920

47. Chen W, Gong L, Guo Z, Wang W, Zhang H, Liu X, et al. A novel integrated method for large-scale detection, identification, and quantification of widely targeted metabolites: application in the study of rice metabolomics. Molecula Plant. 2013; 6(6):1769–1780. https://doi.org/10.1093/mp/sst080 PMID: 23702596

48. Ballabio D, Consonni V. Classification tools in chemistry. Part 1: linear models. PLS-DA. Analytical Methods. 2013; 5(16):3790–3798. https://doi.org/10.1039/C3AY40582F

49. Zhao Q, Xiang X, Liu D, Yang A, Wang Y. Tobacco transcription factor *NtbHLH123* confers tolerance to cold stress by regulating the *NtCBF* pathway and reactive oxygen species homeostasis. Frontiers in Plant Science. 2018; 9:381. https://doi.org/10.3389/fpls.2018.00381 PMID: 29643858

50. Pérez-Rodríguez P, Riano-Pachon DM, Corrêa LGG, Rensing SA, Kersten B, Mueller-Roeber B. PlnTFDB: updated content and new features of the plant transcription factor database. Nucleic acids research. 2010; 38(suppl_1):D822–D827. https://doi.org/10.1093/nar/gkp805 PMID: 19858103

51. Nakagami H, Pitzschke A, Hirt H. Emerging MAP kinase pathways in plant stress signalling. Trends in plant science. 2005; 10(7):339–346. https://doi.org/10.1016/j.tplants.2005.05.009 PMID: 15953753

52. Solanke AU, Sharma AK. Signal transduction during cold stress in plants. Physiology and Molecular Biology of Plants. 2008; 14(1–2):69–79. https://doi.org/10.1007/s12298-008-0006-2 PMID: 23572874

53. Janská A, Maršík P, Zelenková S, Ovesná J. Cold stress and acclimation–what is important for meta-bolic adjustment? Plant Biology. 2010; 12(3):395–405. https://doi.org/10.1111/j.1438-8677.2009.00299.x

54. Carpaneto A, Ivashikina N, Levchenko V, Krol E, Jeworutzki E, Zhu JK, et al. Cold transiently activates calcium-permeable channels in *Arabidopsis* mesophyll cells. Plant physiology. 2007; 143(1):487–494. https://doi.org/10.1104/pp.106.090928 PMID: 17114272

55. DeFalco TA, Bender KW, Snedden WA. Breaking the code: Ca^{2+} sensors in plant signalling. Biochemi-cal Journal. 2010; 425(1):27–40. https://doi.org/10.1042/BJ20091147 PMID: 20001960

56. Hershkovitz V, BEN-DAYAN C, Raphael G, PASMANIK-CHOR M, Liu J, Belausov E, et al. Global changes in gene expression of grapefruit peel tissue in response to the yeast biocontrol agent *Metschni-kowia fructicola*. Molecular plant pathology. 2012; 13(4):338–349. https://doi.org/10.1111/j.1364-3703.2011.00750.x PMID: 22017757

57. Wang J, Pan CT, Wang Y, Ye L, Wu J, Chen LF, et al. Genome-wide identification of MAPK, MAPKK, and MAPKKK gene families and transcriptional profiling analysis during development and stress response in cucumber. BMC genomics. 2015; 16(1):386. https://doi.org/10.1186/s12864-015-1621-2 PMID: 25976104

58. Li K, Yang FB, Zhang GZ, Song SF, Li Y, Ren DT, et al. AIK1, a mitogen-activated protein kinase, mod-ulates abscisic acid responses through the MKK5-MPK6 kinase cascade. Plant physiology. 2017; 173(2):1391–1408. https://doi.org/10.1104/pp.16.01386 PMID: 27913741

59. Teige M, Scheikl E, Eulgem T, Dóczi R, Ichimura K, Shinozaki K, et al. The MKK2 pathway mediates cold and salt stress signaling in *Arabidopsis*. Molecular cell. 2004; 15(1):141–152. https://doi.org/10.1016/j.molcel.2004.06.023 PMID: 15225555

60. Asai T, Tena G, Plotnikova J, Willmann MR, Chiu WL, Gomez-Gomez L, et al. MAP kinase signalling cascade in *Arabidopsis* innate immunity. Nature. 2002; 415(6875):977–983. https://doi.org/10.1038/415977a PMID: 11875555

61. Deng QW, Luo XD, Chen YL, Zhou Y, Zhang FT, Hu BL, et al. Transcriptome analysis of phosphorus stress responsiveness in the seedlings of Dongxiang wild rice (*Oryza rufipogon* Griff.). Biological research. 2018; 51(1):7. https://doi.org/10.1186/s40659-018-0155-x PMID: 29544529

62. Haider MS, Kurjogi MM, Khalil-Ur-Rehman M, Fiaz M, Pervaiz T, Jiu S, et al. Grapevine immune signal-ing network in response to drought stress as revealed by transcriptomic analysis. Plant Physiology and Biochemistry. 2017; 121:187–195. https://doi.org/10.1016/j.plaphy.2017.10.026 PMID: 29127881

63. Abdel-Moneim AM, Al-Kahtani MA, El-Kersh MA, Al-Omair MA. Free radical-scavenging, anti-inflam-matory/anti-fibrotic and hepatoprotective actions of taurine and silymarin against CCl4 induced rat liver damage. PLoS ONE. 2015; 10(12):e0144509. https://doi.org/10.1371/journal.pone.0144509 PMID: 26659465

64. Sivankalyani V, Sela N, Feygenberg O, Zemach H, Maurer D, Alkan N. Transcriptome dynamics in mango fruit peel reveals mechanisms of chilling stress. Frontiers in Plant Science. 2016; 7:1579. https://doi.org/10.3389/fpls.2016.01579 PMID: 27812364

65. Ahmad P, Abd Allah EF, Alyemeni MN, Wijaya L, Alam P, Bhardwaj R, et al. Exogenous application of calcium to 24-epibrassinosteroid pre-treated tomato seedlings mitigates NaCl toxicity by modifying

ascorbate-glutathione cycle and secondary metabolites. Scientific Reports. 2018; 8(1):13515. https://doi.org/10.1038/s41598-018-31917-1 PMID: 30201952

66. Choudhury FK, Rivero RM, Blumwald E, Mittler R. Reactive oxygen species, abiotic stress and stress combination. Plant Journal. 2017; 90(5):856–867. https://doi.org/10.1111/tpj.13299 PMID: 27801967

67. Meloni DA, Oliva MA, Martinez CA, Cambraia J. Photosynthesis and activity of superoxide dismutase, peroxidase and glutathione reductase in cotton under salt stress. Environmental and Experimental Botany. 2003; 49(1):69–76. https://doi.org/10.1016/S0098-8472(02)00058-8

68. Djilianov D, Georgieva T, Moyankova D, Atanassov A, Shinozaki K, Smeeken S, et al. Improved abiotic stress tolerance in plants by accumulation of osmoprotectants-gene transfer approach. Biotechnology & Biotechnological Equipment. 2005; 19(sup3):63–71. https://doi.org/10.1080/13102818.2005.10817287

69. Zhang Y, Li D, Zhou R, Wang X, Dossa K, Wang L, et al. Transcriptome and metabolome analyses of two contrasting sesame genotypes reveal the crucial biological pathways involved in rapid adaptive response to salt stress. BMC plant biology. 2019; 19(1):66. https://doi.org/10.1186/s12870-019-1665-6 PMID: 30744558

70. Klíma M, Vítámvás P, Zelenková S, Vyvadilová M, Prášil IT. Dehydrin and proline content in *Brassica napus* and *B. carinata* under cold stress at two irradiances. Biologia plantarum. 2012; 56(1):157–161. https://doi.org/10.1007/s10535-012-0034-1

71. Lv WT, Lin B, Zhang M, Hua XJ. Proline accumulation is inhibitory to *Arabidopsis* seedlings during heat stress. Plant Physiology. 2011; 156(4):1921–1933. https://doi.org/10.1104/pp.111.175810 PMID: 21670222

72. Janská A, Zelenková S, Klima M, Vyvadilova M, Prášil T. Freezing tolerance and proline content of in vitro selected hydroxyproline resistant winter oilseed rape. Czech journal of genetics and plant breeding. 2010; 46(1):35–40. https://doi.org/10.17221/52/2009-CJGPB

73. Miao ZY, Xu W, Li DF, Hu XN, Liu J, Zhang RX, et al. De novo transcriptome analysis of *Medicago falcata* reveals novel insights about the mechanisms underlying abiotic stress-responsive pathway. BMC genomics. 2015; 16(1):818. https://doi.org/10.1186/s12864-015-2019-x PMID: 26481731

74. Yang O, Popova OV, Süthoff U, Lüking I, Dietz KJ, Golldack D. The *Arabidopsis* basic leucine zipper transcription factor *AtbZIP24* regulates complex transcriptional networks involved in abiotic stress resistance. Gene. 2009; 436(1–2):45–55. https://doi.org/10.1016/j.gene.2009.02.010 PMID: 19248824

75. Song YP, Ci D, Tian M, Zhang DQ. Comparison of the physiological effects and transcriptome responses of Populus simonii under different abiotic stresses. Plant molecular biology. 2014; 86(1–2):139–156. https://doi.org/10.1007/s11103-014-0218-5 PMID: 25002226

76. Rasmussen S, Barah P, Suarez-Rodriguez MC, Bressendorff S, Friis P, Costantino P, et al. Transcriptome responses to combinations of stresses in *Arabidopsis*. Plant physiology. 2013; 161(4):1783–1794. https://doi.org/10.1104/pp.112.210773 PMID: 23447525

77. Walworth AE, Rowland LJ, Polashock JJ, Hancock JF, Song Gq. Overexpression of a blueberry-derived *CBF* gene enhances cold tolerance in a southern highbush blueberry cultivar. Molecular breeding. 2012; 30(3):1313–1323. https://doi.org/10.1007/s11032-012-9718-7

78. Peng T, Guo C, Yang J, Xu M, Zuo J, Bao MZ, et al. Overexpression of a Mei (*Prunus mume*) CBF gene confers tolerance to freezing and oxidative stress in *Arabidopsis*. Plant Cell, Tissue and Organ Culture 2016; 126(3):373–385. https://doi.org/10.1007/s11240-016-1004-7

79. Byun MY, Lee J, Cui LH, Kang Y, Oh TK, Park H, et al. Constitutive expression of *DaCBF7*, an Antarctic vascular plant *Deschampsia antarctica* CBF homolog, resulted in improved cold tolerance in transgenic rice plants. Plant Science. 2015; 236:61–74. https://doi.org/10.1016/j.plantsci.2015.03.020 PMID: 26025521

80. Jiang JJ, Ma SH, Ye NH, Jiang M, Cao JS, Zhang JH. WRKY transcription factors in plant responses to stresses. Journal of integrative plant biology. 2017; 59(2):86–101. https://doi.org/10.1111/jipb.12513 PMID: 27995748

81. Wang Y, Shu Z, Wang W, Jiang X, Li D, Pan J, et al. *CsWRKY2*, a novel *WRKY* gene from *Camellia sinensis*, is involved in cold and drought stress responses. Biologia plantarum. 2016; 60(3):443–451. https://doi.org/10.1007/s10535-016-0618-2

82. Fujita M, Fujita Y, Maruyama K, Seki M, Hiratsu K, Ohme-Takagi M, et al. A dehydration-induced NAC protein, RD26, is involved in a novel ABA-dependent stress-signaling pathway. The Plant Journal. 2004; 39(6):863–876. https://doi.org/10.1111/j.1365-313X.2004.02171.x PMID: 15341629

83. Xie YP, Chen PX, Yan Y, Bao CN, Li X, Wang LP, et al. An atypical R2R3 MYB transcription factor increases cold hardiness by CBF-dependent and CBF-independent pathways in apple. New Phytologist. 2018; 218(1):201–218. https://doi.org/10.1111/nph.14952 PMID: 29266327

84. Wang YJ, Zhang ZG, He XJ, Zhou HL, Wen YX, Dai JX, et al. A rice transcription factor OsbHLH1 is involved in cold stress response. Theoretical and Applied Genetics. 2003; 107(8):1402–1409. https://doi.org/10.1007/s00122-003-1378-x PMID: 12920519

85. Ramsay NA, Glover BJ. MYB-bHLH-WD40 protein complex and the evolution of cellular diversity. Trends in plant science. 2005; 10(2):63–70. https://doi.org/10.1016/j.tplants.2004.12.011 PMID: 15708343